ACS OMEGA

Open Access

http://pubs.acs.org/journal/acsodf

Article

Antiangiogenic Potential of Beneficial Sterols from Parotoid Gland Secretion of Indian Common Toads (*Duttaphrynus melanostictus*) in the Coastal Region of the Indian Subcontinent: An *In Vivo* to *In Silico* Approach

Sandhya Maji,* Susanta Sadhukhan, Arup Kumar Pattanayak, and Jayanta Kumar Kundu*

Cite This: *ACS Omega* 2025, 10, 10480−10492

Read Online

ACCESS | Metrics & More | Article Recommendations | Supporting Information

ABSTRACT: The toxins of the Bufonid toads have been used formerly as ethnomedicine to treat different diseases, including chronic hepatitis, hypertension, and multiple cancers. Thus, toads' venom has a great impact on traditional health care. However, the main emphasis of this study is to identify natural components present in toad parotoid gland secretion and evaluate their antiangiogenic effects. Sterol-rich extracts of parotoid gland secretions were isolated in an ethyl acetate medium from a natural population of Indian common toads (*Duttaphrynus melanostictus*) from the coastal region (Purba Medinipur, West Bengal) of the Indian subcontinent. The antiangiogenic activity was assessed using a chick embryo chorioallantoic membrane (CAM) assay. Gas chromatography−mass spectrometry (GC−MS) analysis was conducted to determine the chemical composition. *In silico* molecular docking was subsequently employed to detect putative biologically active substances with antiangiogenic potential. The majority of the sterol components were identified and mainly cholesterol was found at the greatest concentration (31.10%). According to the quantitative analysis Campesterol (15.73%), γ-sitosterol (10.09%), lathosterol (2.79%), stigmasterol (0.933%), and brassicasterol (0.466%) were also present. According to the outcome of the CAM assay, there was 51.62% suppression of blood vessel formation when compared to the untreated. Bonferroni's posthoc test analysis revealed a statistically significant difference at $p < 0.001$. Using GraphPad Prism software 8.1.2, nonlinear regression analysis yielded EC_{50} values of 24.27 μg/mL. Following identification, the primary bioactive chemicals in the extract under investigation showed a more robust interaction with vascular endothelial growth factor receptors (VEGFRs) *in silico* molecular docking experiments. To the best of our knowledge, this is the first-hand report on the ethyl acetate extract (sterol-rich) of parotid gland secretion from the Indian common toad showing antiangiogenic activity by targeting VEGFRs. However, the findings of this study suggest that the bioactive compound from the investigated extract can be considered for the development of antiangiogenic medicine.

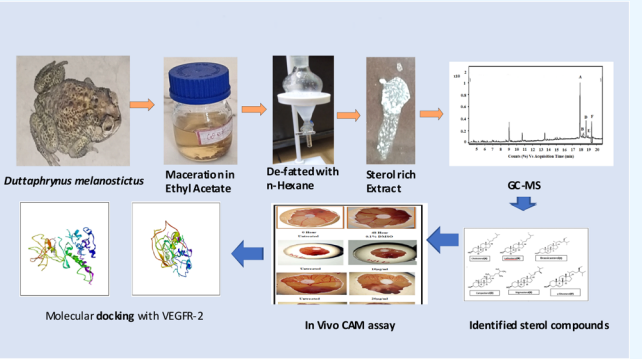

INTRODUCTION

The formation of new blood vessels from pre-existing blood vessels is called angiogenesis. Initially, the Pro-angiogenic factors concentration gradient controls the activation and migration of endothelial cells which then attach to the blood vessels, and initiate the formation of new blood vessels.[1] This neovascularization is crucial for tumor growth beyond 1−2 mm in diameter.[2,3] Neovascularization is the most important route for the invasion of cancer cells, metastasis, and the growth of tumors. The prevention of this angiogenesis process may create hindrances for the progression of cancer. Many antiangiogenic compounds have since been developed to prevent the development or propagation of cancer.[4] Throughout the globe, research is being carried out to discover drugs that combat antiangiogenic cancer, particularly using natural compounds. The treatment of numerous illnesses has made substantial use of natural ingredients or their derivatives.[5,6] Several scientists have proposed using animal body parts and metabolic byproducts (biological secretions and excrements) in combined therapy to block angiogenesis.[7] The fact that human populations from various nations have employed the amphibian species bufonid toad to treat illnesses is indicative of their significance in traditional medicine.[8,9] Interestingly, in the past,

Received: November 28, 2024
Revised: January 24, 2025
Accepted: January 28, 2025
Published: March 4, 2025

China used to make anticancer curable ethnomedicine from the venom of the common Asian toad species, *Bufo gagrarians* Cantor, 1842, and *Bufo melanostictus* (Schneider, 1799)[10]

A sterilized hot water extract of the dried skin of the toad *Bufo gargarizans*, and traditional Vietnamese medication isolated from *B. melanostictus*, demonstrated notable effects on malignant tumors, including esophagal and liver cancers.[11−14] Moreover, several chemical components possessing diverse biological activities have been extracted from these extracts, such as bufadienolides, cyclic amides, indole alkaloids, and polypeptides, with bufadienolides being the primary active component. Recent research has also demonstrated the anticancer activity of certain bufadienolides, as demonstrated by bufalin, bufotalin, Gama bufotalin, cinobufotalin, and cinobufagin.[15−26] Previous investigations on *B. melanostictus*-antineoplastic factor 1 (BM-ANF1) from common Indian toad (*B. melanostictus* Schneider) has reported strong antitumor and cytotoxic activity.[27−29] Selected physiological actions of the crude toad toxin or purified bioactive components of the Bufonid family have been reported in very few publications.

However, the majority of earlier chemical investigations used toad venom extracts in the forms of ethanol, water, and methanol. The ethyl acetate extract of parotoid gland secretions from Indian common toads (natural population), particularly those from the Indian subcontinent's coastal area (Purba Medinipur, W.B.), remains unknown for having antiangiogenic activity. The current work aims to employ GC−MS to identify a combination of bioactive chemicals, mostly sterol compounds, in an ethyl acetate extract of parotoid gland secretion (PGS) from Indian common toads. The less harmful antiangiogenic potentials were subsequently evaluated. Using an *in silico* method, the mechanisms of action of the main sterols produced from the extract mentioned above on vascular endothelial growth factor receptors (VEGFRs-VEGFR1, VEGFR2, and VEGFR3) were investigated because VEGF (vascular endothelial growth factor) is the most prominent inducer of angiogenesis by binding to its receptors (VEGFR1 and VEGFR2) on the endothelial cells, thus activating the cascade of many downstream signaling pathways essential for angiogenesis. Thus, VEGFR inhibitors (e.g., small molecule tyrosine kinase inhibitors like sorafenib, sunitinib, and monoclonal antibodies like bevacizumab) are commonly used in cancer therapy to block blood supply to tumors. The main sterols were also tested for their toxic effects and mutagenicity.

MATERIALS AND METHODS

Chemicals and Reagents. All of the chemicals and solvents were of analytical grade. Ethyl acetate (Cat. No. 1096231000) and dimethyl sulfoxide (DMSO) (Cat. No. 1029521000) were purchased from Merck (Darmstadt, Germany).

Secretion Collection and Extraction. The collection of parotoid gland secretion from the Indian common toad was carried out in their natural habitat by manual compression of both parotoid glands, which are located behind their eyes. The secretions were collected in an ice jacket container from Indian common toads distributed in the agricultural land (87° 44′ 36.6″ E, 21° 5.1′ 10.6″ N), located in the coastal region (Purba Medinipur) of the Indian subcontinent, during May 2023. After collection, the animals were released to their natural habitat without any harm, and collected secretions were extracted with ethyl acetate by the cold maceration technique. The ethyl acetatesoluble extract was filtered by Whatman paper No. 1 and concentrated in vacuo. Then, the resultant sample was prepared for GC−MS analysis and chick embryo chorioallantoic membrane (CAM) assay by making a concentration of 1 mg/mL. The study was approved by the University Ethics Committee of Vidyasagar University, Paschim Medinipur (Ethical No. VU/IAEC/CPCSEA/12/7/2022 dated 22.11.2022).

GC−MS Analysis. An Agilent 6890B gas chromatograph (Agilent Technologies) coupled with a tandem quadrupole mass spectrometer and a multipurpose sampler (Gerstel, Germany) was used to perform GC studies of the ethyl acetate extract of PGS. The Restek MXT-1 capillary column (crossbond 100% dimethyl polysiloxane; 30 m × 250 mm × 0.25 mm; Restek) was used for the GC tests. The injection was carried out in the splitless mode at 28 °C for 0.75 min of split valve off-time. Helium, the carrier gas, was employed at a steady flow rate of 1.1 m/min. The temperature of the column oven was configured to range from 35 to 285 °C, with a 5 min maintenance period and a 10 °C/min increase to 280 °C for 10.5 min. The final temperature was set at 50 °C/min to 285 °C and maintained for 29.9 min. The electron impact (EI) ion source was set at 23 °C with electron energy of 70 eV. The solvent cutoff time was set to 3 min with full scan mode (m/40−800 Da). Collision energies were set to 5, 10, 15, and 20 eV for each run. The nitrogen flow was set at 1.5 mL/min, and the helium flow was set at 2.25 mL/min. The product ion scan ranged from 40 to 400 Da. The bioactive components of PGS were identified using relative retention times and a database search in commercial mass spectrum databases of the National Institute of Standards and Technology (NIST-17). The Agilent Mass Hunter quantification software (Version B.07.00) was utilized for data analysis.

CAM Assay. The effect of parotoid gland secretion on angiogenesis was assessed using the CAM assay as described before.[30−32] The primary benefits of the CAM model include high vascularization qualities, great repeatability, simplicity, and cost-effectiveness. Experiments on chicken embryos did not require approval from the institutional animal ethics committee. In brief, 3-day-old fertilized chick eggs were purchased from a nearby hatchery (A.R.D. Department State Poultry Farm R.K.V.Y Project, C8H6+PPM, Midnapore Railway Station Rd, Midnapore, West Bengal 721101). They were weighed, and following that, the eggs were cleaned with 70% ethanol to remove contamination from the eggshell. The eggs were then incubated at 37 °C for 48 h under constant humidity. The egg tray was automatically tilted for a 45° angle every 30 min, mimicking the natural process. On the fifth day of incubation, using the process of candling, viable eggs with moving embryos were separated and the unfertilized eggs were discarded. A scalpel was used to make a small window (1 × 1 cm) on the wide end of the eggs, where the air sac is located at the fifth day of incubation. 2−3 mL of albumin was withdrawn. Fertilized eggs were divided into four groups of six eggs each; Group 1: Control (0.01% DMSO), Group 2: 10 μg/mL of sterol extract, Group 3: 20 μg/mL of sterol extract, and Group 4: 25 μg/mL of sterol extract. On the seventh day of incubation, a sterile disc (6 mm) piece was inserted into the chorioallantoic membrane through an opened small square window of an egg.

The ethyl acetate extracts were dissolved in DMSO (0.1% v/v) and placed onto a sterile Whatman paper disc (6 mm) at various concentrations (10, 20, and 25 μg/mL). Sterile paper disks containing 0.1% DMSO were used as both the compound's vehicle and the control. The sterile Whatman paper disks, impregnated with the desired concentration, were then aseptically placed in the CAM. The window aperture was

https://doi.org/10.1021/acsomega.4c10809
ACS Omega 2025, 10, 10480−10492

Table 1. Main Compounds of Sterol-Containing Extract of Parotoid Gland Secretion in Indian Common Toad, as Determined by GC−MS

sl. no	compound name	cas no.	RT	area of %	MW	MF	score NIST LIB (2017)%
1	cholesterol	57-88-5	17.957	31.1	386.7	$C_{27}H_{46}O$	87.15
2	lathosterol	80-99-9	18.095	2.79	386.7	$C_{27}H_{46}O$	72.14
3	brassicasterol	474-67-9	18.433	0.466	398.7	$C_{28}H_{46}O$	71.89
4	campesterol	474-62-4	18.706	13.06	400.7	$C_{28}H_{46}O$	80.17
5	stigmasterol	83-48-7	18.875	0.933	412.7	$C_{29}H_{48}O$	78.28
6	γ-sitosterol	83-47-6	19.416	11.19	414.7	$C_{29}H_{50}O$	87.82
7	1,2-benzenedicarboxylic acid, monononyl ester	57-10-3	9.113	3.03	256.43 g/mol	$C_{17}H_{24}O_4$	71.38
8	octadecanoic acid	57-11-4	10.697	1.85	284.5 g/mol	$C_{18}H_{36}O_2$	88.77
9	2′-(trimethylsilyl)oxy-2,3,6′-trimethoxychalcone		15.27	0.0528	330.3 g/mol	$C_{21}H_{26}O_5Si$	58.77

subsequently sealed using adhesive tape, and the eggs were incubated for 48 h at 37 °C with a constant humidity of 85%. After 48 h, the eggs were opened, and the CAMs were photographed using a digital camera. The experiments were repeated three times, with four eggs per condition. Before and after treatment, images of the same CAM's surface within the same test sample were contrasted. Representative images were analyzed using the web-based WimasisWim CAM service (Wimasisa GmbH, Munich, Germany) to measure angiogenesis (https://www.wimasis.com/tube-formation-assay). The anti-angiogenic effect was then calculated using the following formula:

$$\%\ \text{inhibition} = \text{score of control vessels} - \text{score of treated vessels} \times 100/\text{score of control vessels}$$

The toad sample collection and CAM assay images were obtained by using an Oppo Reno Pro 5G (50MP Sony imx890 with an OIS camera; Oppo Mobiles India Private Ltd., India).

Molecular Docking. The Auto Dock 4.2 program was used to dock the major bioactive compounds of PGS,[33] campesterol, and γ-sitosterol against the human VEGFR1 (3HNG), VEGFR2 (3EWH), and VEGFR3 (4BSJ) molecular target to identify potential inhibitors.[34−36] The three-dimensional (3D) structures from PubChem were used to prepare the ligands and the Open Babel GUI (Graphical user interface) was used to convert them to the Protein Data bank (PDB) format.[37] Auto Dock version 4.2 was used for protein (PDB ID: 3EWH) that was downloaded from the Research Collaboratory for Structural Bioinformatics (RCSB) PDB optimization through the removal of water and other atoms, the addition of a polar hydrogen group, and then the assignment of Kollman energy.[72] The following predetermined parameters were used for the Lamarckian genetic algorithm-based molecular docking process: a maximum of 2,500,000 energy evaluations, a mutation rate of 0.02, a crossover rate of 0.8, and an initial population of 150 randomly assigned individuals. For every ligand target docking, 50 independent runs were carried out. To achieve the best binding, the pose of the reduced native ligand which shows a great deal of similarity to the original cocrystallized ligand, the grid box was optimized.[38] Docking parameter validation was based on the residues included in the docking interaction, the root-mean-square deviation (RMSD) value, and the generated pose. The most appropriate binding conformations were chosen based on the lowest values of the free energy of binding (ΔG) and inhibition constant (K_i). The root-mean-square deviation value was found to be less than 2∧A between the native cocrystal and the docked positions. Biovia Discovery Studio Visualizer 2019 was used to study the molecular interactions between the target protein and chosen ligands at their lowest binding energy pose.[39]

Drug-Likeness Prediction with ADMET. To determine each compound's Absorption Distribution Metabolism Excretion and Toxicity (ADMET) attributes, the simplified molecular input line entry system (SMILES) was copied from PubChem and entered into the chem-informatics online tools SwissADME[40] and pkCSM.[41,42] SwissADME also predicted Lipinski parameters and drug-likeness.[40−42]

Statistical Analysis. The means ± standard deviation (SD) of the results are displayed. A one-way analysis of variance (ANOVA) followed by the Bonferroni posthoc test was used to assess the statistical significance. Using GraphPad Prism software 8.1.2, nonlinear regression analysis was used to determine the EC_{50} values, or concentrations, that caused 50% inhibition in blood vessel proliferation. Statistical significance was indicated by a p-value of less than 0.05.

RESULTS

GC−MS analysis was employed to examine the major bioactive substances present in the ethyl acetate extract of parotoid gland secretion obtained from a natural population of Indian common toads. GC−MS analysis in the ethyl acetate polar solvent medium revealed that different sterols, such as cholesterol (31.1%), lathosterol (2.79%), brassicasterol (0.466%), campesterol (13.06%), stigmasterol (0.933%), and γ-sitosterol (11.19%), are present in the parotoid gland secretion from a natural population of Indian common toad. Sterols were seen between 17 and 20 min in terms of retention times. Molecular ion (m/z) values, information from published sources, and information from the GC−MS (NIST) library were used to identify these sterols (Table 1 and Figure 1). The chemical structures of the identified compounds are shown in Figure 3. Lathosterol and γ-sitosterol were identified for the first time in the parotoid gland secretion of the natural population of Indian common toads.

Antiangiogenic Activity of the Sterol-Containing Extract of Parotoid Gland Secretion. Different concentrations were used to determine the antiangiogenesis effect of the sterol-containing extract from parotoid gland secretion (Figure 3A) and established by the more efficient antiangiogenic screening CAM assay. The antiangiogenic effect of the tested compound was evaluated through image analysis using the WimCam software program (Figure 3B), where inhibition of angiogenesis was evaluated based on four parameters: percentage of vessel density, total vessel network length, total segments, and sprouting ability indicated by total branching. The CAM assay was performed using three concentrations of 10,

https://doi.org/10.1021/acsomega.4c10809
ACS Omega 2025, 10, 10480−10492

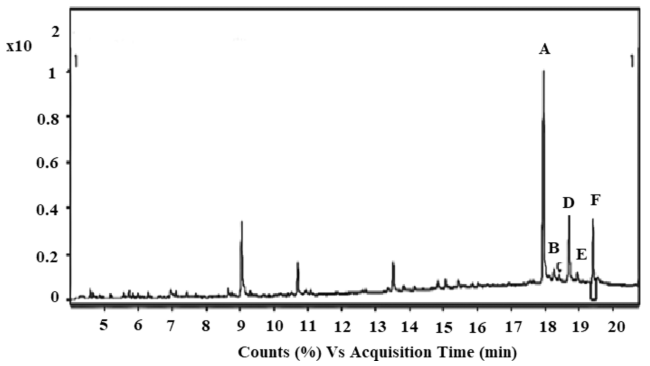

Figure 1. GC−MS chromatogram for the ethyl acetate extract of parotoid gland secretion in Indian common toad indicates the abundance of sterol compounds. The peak is denoted by letters A: cholesterol, B: lathosterol, C: brassicasterol, D: campesterol, E: stigmasterol, and F: γ-sitosterol.

20, and 25 μg/mL with 10 μL volume of each concentration inoculated per egg. Extracts at 10 20, and 25 μg/mL exhibited 24.39, 30.81, and 51.62% inhibition at statistical significance at $p < 0.01$ and $p < 0.001$, respectively, when compared with the untreated sample (Figure 4).

According to these observations, the ethyl acetate extract of parotoid gland secretion exhibits a significant dose-dependent reduction (Table 2). Our study found that the EC_{50}-24.27 μg/mL of ethyl acetate extract inhibited the development of blood vessels.

Table 2. Effect of the Sterol-Containing Extract on the Chorioallantois Membrane Angiogenesis Assay

concentration	blood vessel density (%)	% of inhibition	EC_{50}
untreated	24.62 ± 0.2630		
VC control (0.1% DMSO)	26.9 ± 0.4956	9.30%	24.27 μg/mL
10 μg/mL	18.6 ± 0.6316	24.39%	
20 μg/mL	17.1 ± 0.9003	30.48%	
25 μg/mL	11.9 ± 0.7993	51.62%	

Molecular Docking. Two major bioactive compounds (campesterol and γ-sitosterol) of parotoid gland secretion identified by GC−MS analysis from an Indian common toad were selected and subjected to molecular docking with VEGFR-1(3HNG), VEGFR-2(3EWH), and VEGFR-3(4BSJ). Axitinib was used as a standard control. The docking results of bioactive compounds are shown in (Figures 5−7). The docking results are represented in the form of minimum binding energy values, K_i values, H-bond, and hydrophobic interactions and are tabulated in (Tables 3−5). The hydrophobic amino acids (Lys861 Glu878, Cys912, and Asp1040) of the intracellular domain of VEGFR1 are recognized as the key drug-binding residues responsible for the maintenance of inhibitor activity.[43] Interestingly, the interaction profile of axitinib interacted hydrophobically with Lys861 and Asp1046 and formed a hydrogen bond with Cys912 while γ-sitosterol formed a hydrophobic interaction with Lys861 and campesterol formed a conventional hydrogen bond with Asp1046 and hydrophobically interacted with cys912. The binding energies of γ-sitosterol and campesterol were −12.04 and −9.94 kcal/mol, greater than axitinib (−9.5 kcal/mol). The inhibition constants (K_i) of γ-sitosterol and campesterol were 1.49 and 52.07 nM, less than the

Table 3. Binding Interactions of Major Sterol Compounds along with Standard Inhibitors with VEGFR1 (PDB-3HNG)—Docking and Interaction Analysis

compound	protein (PDB ID)	binding energy, ΔG (kcal/mol)	inhibition constant KI (nM)	H-bond	ligand interaction
axitinib	3HNG	−9.5	108.09	Cys912(1-H), Asn919(1-H), Asn916(1-H),	Val 909, Val 892, Phe 1041, Ala 859, Val 841, Leu 833, Cys 912, Asn 919, Asn 916
campesterol	3HNG	−9.94	52.07	Asp 1040(1-H)	Cys 912, Asp 1040, Val 892, Val 909, Cys 1039, Leu 1029, Try 911, Ala 855, Phe 1044, Leu 833
γ-sitosterol	3HNG	−12.04	1.49	Ile 1019 (1-H), Arg 1021(1-H)	Leu 882, Cys 1018, Cys 1059, Val 892, Val 841, Phe 1041, His 1020, Ile 881

https://doi.org/10.1021/acsomega.4c10809
ACS Omega 2025, 10, 10480−10492

Table 4. Binding Interactions of Major Sterol Compounds along with Inhibitors with VEGFR2 (PDB-3EWH)—Docking and Interaction Analysis

compound	protein (PDB ID)	binding energy, ΔG (kcal/mol)	inhibition constant KI (nM)	H-bond	ligand interaction
axitinib	3 EWH	−8.76	380.53	Glu 885 (1-H)	Val 848, Ala 866, Phe 1047, Lys 868, Thr 916, Asp 1046, Val 914, Glu 885, Leu 889
campesterol	3 EWH	−10.68	14.93	Cys 919 (2-H), Glu 917(1-H)	Cys 919, Glu 917, Val 899,Thr 916, Lys 868, Gly 843
γ-sitosterol	3 EWH	−11.04	8.13	Cys 919 (1-H) LyS 920 (1-H)	Cys 919, Lys 920, Glu 885, Asp 1046, Lys 868, Thr 916, Phe 921, Leu 889, Val 899, Leu 840, Val 848, Ala 866, Leu 035, Cys 1045, Phe 918, PhE 1047

Table 5. Binding Interactions of Major Sterol Compounds along with Inhibitors with VEGFR3 (PDB-4BSJ)—Docking and Chimera Analysis

compound	protein (PDB-ID)	binding energy, ΔG (kcal/mol)	inhibition constant KI (nM)	H-bond	ligand interaction
axitinib	4BSJ	−6.01	39430	Ala429 (1-H), Glu426 (1-H), Ser430 (1-H), Ala442 (1-H)	Ala442, Leu443, Thr444, Ile547, Pro432, Ser431, Ala429, Glu426, Ser430, Ala429, His425, Arg545, Tyr435, Thr446, Val511
campesterol	4BSJ	−9.52	105.01	Glu544 (1-H),	Glu544, Lys427, Leu546, Arg545, Ile547, Trp463, Tyr550, Tyr435, Tyr548, Ser433, Pro432, Phe549, ser431
γ-sitosterol	4BSJ	−8.31	815.02	Glu426 (1-H), Arg545 (1-H)	Glu426, Arg545, Tyr550, Pro432, Ile547, Ser430, Ser431, Ala429, Lys427, Tyr550, Tyr548, Trp463

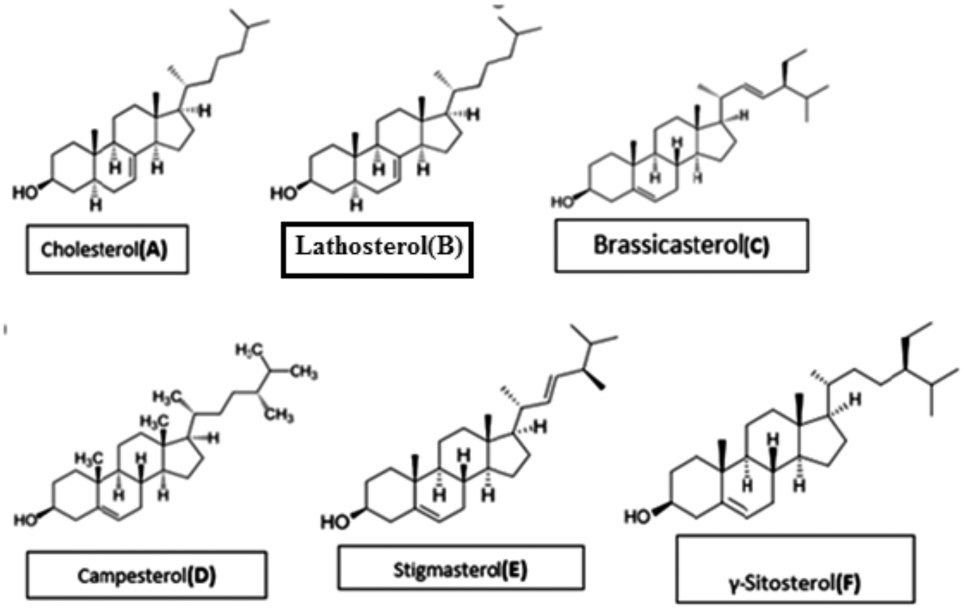

Figure 2. Chemical structure of (A) cholesterol, (B) lathosterol, (C) brassicasterol, (D) campesterol, (E) stigmasterol, and (F) γ-sitosterol (the structures were taken from the https://pubchem.ncbi.nlm.nih.gov).

axitinib (108.09 nM), which indicates that γ-sitosterol and campesterol have relatively higher binding affinity toward VEGFR1. Lys861 forms a major amino acid residue of ATP binding sites in the intracellular domain VEGFR1 and interestingly, both γ-sitosterol and axitinib inhibitors interacted with it. Lys868, Asp1046, Cys919, and Glu885 are recognized as the critical residues on the VEGFR2 kinase domain (PDB ID: 3EWH). The Cys919 residue is the main one responsible for maintaining the inhibitory action.[44] Similar to the cocrystallized ligand k11, campesterol and γ-sitosterol exhibited a conventional hydrogen bond with Cys919, as depicted in. Additionally, k11 had an unfavorable interaction with Glu885 and Asp1046, while γ-sitosterol formed a van der Waals interaction with Glu885 and Asp1046. Axitinib has a conventional hydrogen bond with Glu885. The binding energies of campesterol, γ-sitosterol, and axitinib were −11.04, −10.68, and −8.76 kcal/mol, respectively. The inhibition constants (K_i) of γ-sitosterol, campesterol, and axitinib were 1.49, 52.07, and 108.09 nM, respectively. Our test compound γ-sitosterol, campesterol exhibits higher binding affinity toward VEGFR2 than axitinib. Similar to VEGFR1, Lys868 forms a crucial residue for ATP binding in the case of VEGFR2 which was recognized to show hydrophobic bonding with campesterol and γ-sitosterol and commercial inhibitors, axitinib. Campesterol and γ-sitosterol show strong interactions with VEGFR3 with greater binding energy (−8.31 and −9.52 kcal/mol) and low K_i values (815.02 and 105.01 nM) than established inhibitors (axitinib: binding energy −6.01 kcal/mol and K_i value 39.43 μM).

Drug-Likeliness. The selected major sterols are evaluated for their drug-likelihood properties with the help of the Lipinski

https://doi.org/10.1021/acsomega.4c10809
ACS Omega 2025, 10, 10480−10492

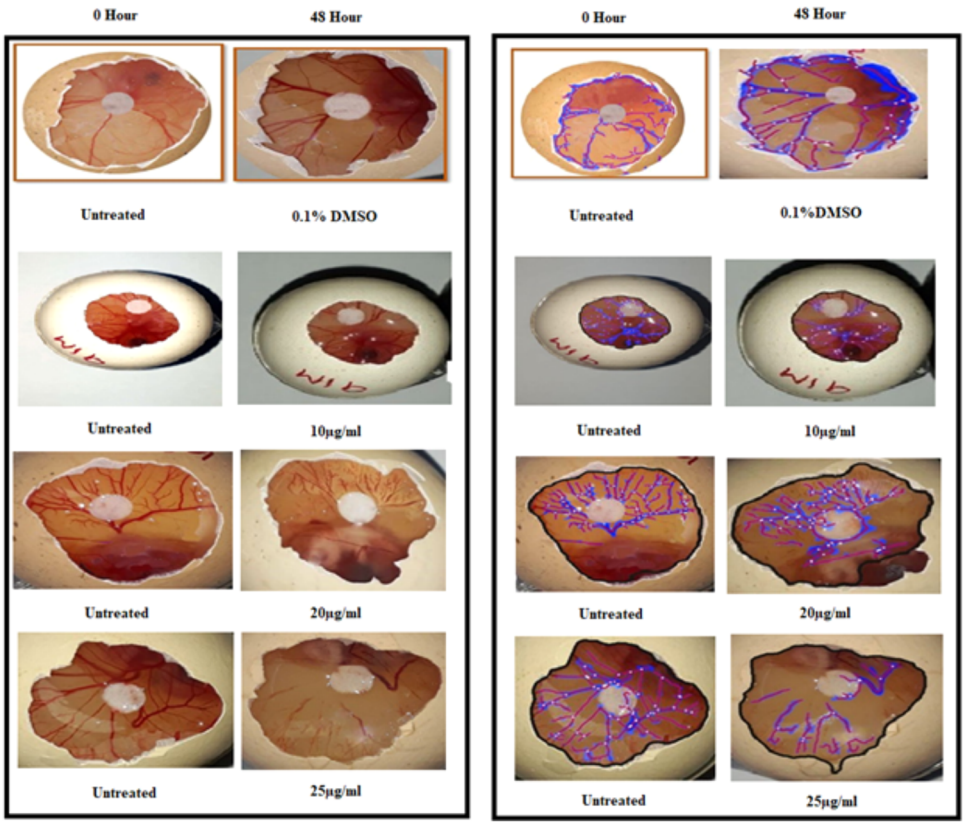

Figure 3. Effect of sterol-containing extract from parotid gland secretion (Indian common toad) on the chick embryo vascular system. (A) Representative images of CAMs at 0 and 48 h after incubation with sterol-containing extract (10, 20, and 25 μg/mL). (B) Wimasis software-generated blood vessel densities in CAM.

rule of five filters. This analysis helps to distinguish between drug-like and nondrug-like molecules. Table refers to the drug-likeness properties of Campesterol and γ-sitosterol, which clearly show that Campesterol and γ-sitosterolpossess good and acceptable drug-likeness properties like molecular weight, flexibility, hydrogen bond donor, hydrogen bond acceptor, and no violation of the Lipinski rule.

ADMET Analysis. Absorption Distribution Metabolism Excretion and Toxicity (ADMET) analysis was performed to understand the pharmacokinetic properties of the compounds.

DISCUSSION

This study mainly assessed the antiangiogenic activity of an ethyl acetate extract of parotoid gland secretion from a natural population of Indian common toads by both *in-vivo* and *in silico* methods. Reports from different studies have demonstrated specific biological actions of the crude toad toxin or purified bioactive components from the bufonid family. However, this is the first study to look into the chemical constituents and antiangiogenic potentials of the ethyl acetate extract of the parotoid gland secretion of Indian common toads, particularly from the Indian subcontinent's coastal region (Purba Medinipur, West Bengal). The venom's chemical composition varies greatly based on the type, the region in which it is produced, and differences in the methods used for collection and processing.[45,46] The solvent extraction approach plays a key role in the separation of compounds with biological activity. The results obtained for the intended activity vary because bioactive substances have varying solubilities in different solvents. A medium-polar solvent, ethyl acetate, is capable of extracting several nonpolar substances. The ethyl acetate extracts of parotoid gland secretion of Indian common toads under investigation showed mostly sterols in the GC−MS results. Compared to bufadienolides, the sterols found in toad venoms have not been investigated as extensively. However, bufonid toads cannot produce sterols independently and are mainly acquired in dietary forms.[47] Six compounds were found to be present, three of which were major components, (Figure 1). By comparison with reference compounds, these components were identified as cholesterol (31.10%), campesterol (15.73%), and γ-sitosterol (10.09%) as major components: Lathosterol (2.79%), brassicasterol (0.466%), and stigmasterol (0.933%) in trace amount. Evidence from earlier research has indicated the presence of γ-sitosterol and cholesterol in the dried venom of Taiwan toads (*Bufo vulguris*).[48] 5−20% γ-sitosterol and a combination of cholesterol have been identified in the sterol fractions of skin extracts from *Bufo vulgaris*, *B. vulgaris formosus*, and *Bufo arenarum*.[49] A sterol fraction was extracted from the Argentine toad (*B. arenarum*)[50] and γ-sitosterol was discovered from the Chinese toad.[51] Only four sterols—cholesterol, brassicasterol, stigmasterol, and campesterol—have been previously detected in Vietnamese toads (*B. melanostictus*).[14] Furthermore, the Vietnamese toad *B. melanostictus* and the Indian common toad (*Duttaphrynus melanostictus*) had a similar sterol profile, except lathosterol being present and γ-sitosterol replacing β-sitosterol (Figure 2). Interestingly, the entire detected sterols compounds in the ethyl acetate extract of the parotoid gland secretion from the Indian common toad (*D. melanostictus*) were recognized as anticancer agents in many previous studies but failed to show the mechanism of

https://doi.org/10.1021/acsomega.4c10809
ACS Omega 2025, 10, 10480−10492

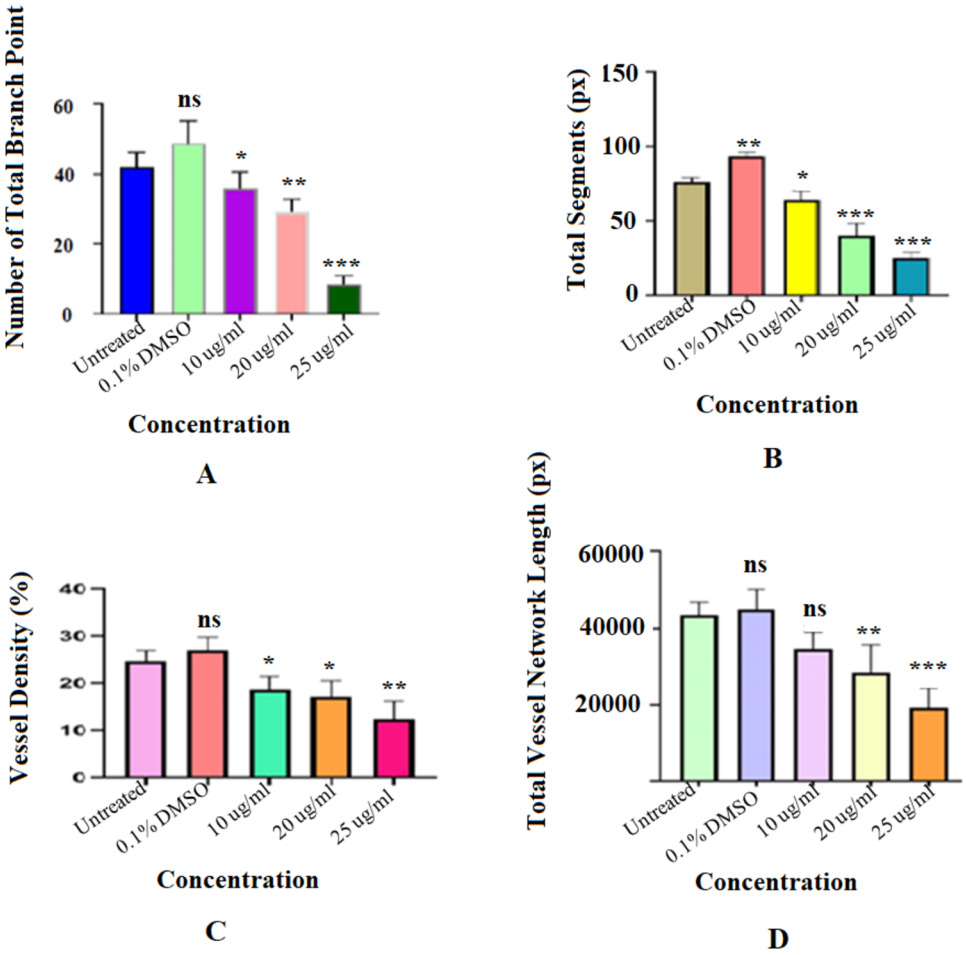

Figure 4. Sterol-containing extract reduced capillary formation in vivo in the chick embryo vascular system. (A) Graph demonstrating the difference in the number of the total branch. (B) Graph demonstrating the total segment. (C) Graph denoting the percentage inhibition in blood vessel density. (D) Total vessel network length and total branch. * indicates statistical significance at $p < 0.05$; ** indicates statistical significance at $p < 0.01$ and *** at $p < 0.001$ compared with the untreated sample.

association.The antiangiogenic effect of sterols from parotoid gland secretion was investigated in vivo utilizing the chick embryo CAM assay. CAM has the advantage of being simple to use and inexpensive. Furthermore, the circulatory system of CAM is directly accessible for observation and research, with no metabolic or hormonal impacts.[52] The quantification of vascular alterations in the CAM in response to angiogenesis inhibition was simplified by comparing images of CAM vessels with and without the application of test chemicals. The qualitative alterations in capillaries for each test sample were used to quantify the antiangiogenic properties of ethyl acetate extracts. In the current investigation, DMSO at a concentration of 0.1% was employed as both the compounds' vehicle and the control. The results of the CAM assay are reported in (Figure 3). It was discovered that the area of the CAM beneath the disc containing 0.1% DMSO (control) did not alter vascular density; the usual branching pattern of blood vessels was seen, demonstrating that disc weight does not affect blood vessel growth. According to these observations, the ethyl acetate extract of parotoid gland secretion exhibits a significant dose-dependent reduction. Our study found that the EC_{50}-24.27 μg/mL (Table 2) of ethyl acetate extract inhibited the development of blood vessels. Thus, it is reasonable to suggest that the high concentrations of sterol compounds in the ethyl acetate extract determined by gas chromatography may contribute to their antiangiogenic properties (Figure 4).

Previous investigations have shown results that can provide support for this deduction. It is reported that the antibacterial, antitumor, cytotoxic, and even immune-promoting properties are present in brassicasterol, stigmasterol, campesterol, and γ-sitosterol. Previous studies[53,54] support the cytotoxicity activities of γ-sitosterol (plant source) against colon and liver cancer cell lines. Additionally, campesterol (plant source) that was present in parotoid gland secretion has been reported in the literature to possess many important pharmacological actions that include anticancer, antiangiogenic, antioxidant, and anti-inflammatory activities.[55−58] For instance, when lathosterol was combined with cholesterol (plant source) and tested against cell lines, it exhibited moderate cytotoxicity which is greater than the individual compound.[59] This conclusion suggested that the identified sterol compounds may be responsible for the observed activity. Antiangiogenic substances may block blood vessels via up- or down-regulating genes that control angiogenesis. One of the best targets for inhibiting angiogenesis is VEGFRs.[60,61] Small compounds that decrease VEGFR's tyrosine kinase activity prevent blood vessel sprouting by blocking downstream signaling pathways associated with VEGFR.[62,63] Over the last several years, the number of VEGFR inhibitors has expanded substantially.[64] Axitinib is one of them; it binds to the three

https://doi.org/10.1021/acsomega.4c10809
ACS Omega 2025, 10, 10480−10492

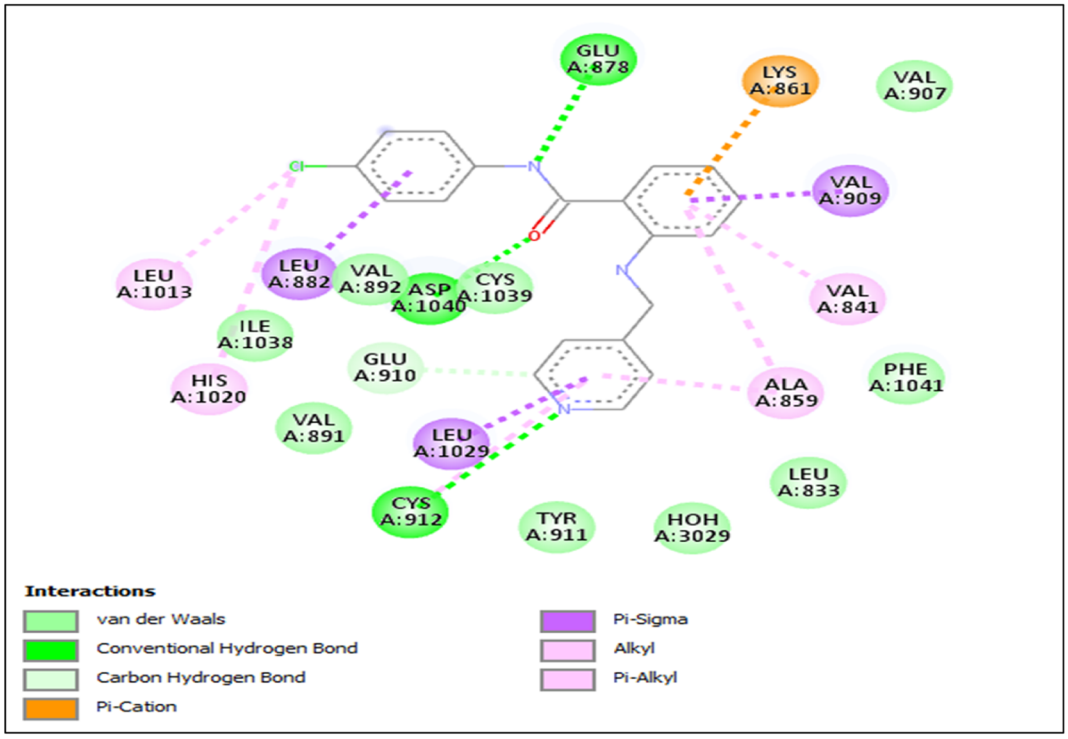

A: 2D interaction of the established inhibitor (axitinib) with VGFR1

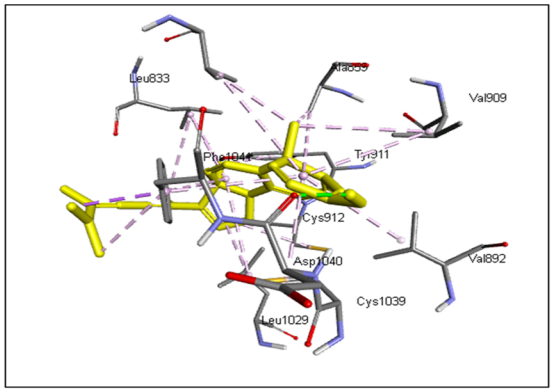

B: 3D-view of interactive residue

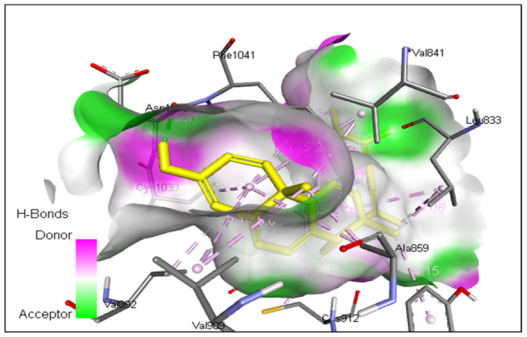

C: 3D- view of H-bond, donor-acceptor residue

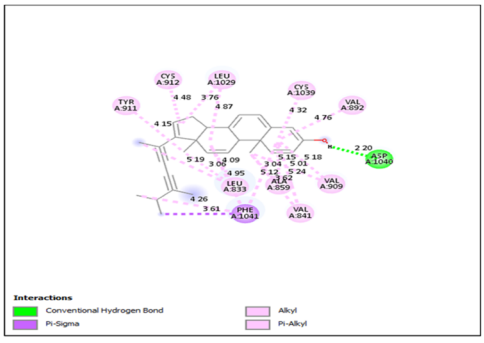

D: 2D diagram of interaction with campesterol

Figure 5. 3D and 2D interaction diagrams of the campesterol with their acceptor VEGFR1 (PDB: 3HNG) and γ-sitosterol with their acceptor VEGFR1 (PDB-3HNG).

https://doi.org/10.1021/acsomega.4c10809
ACS Omega 2025, 10, 10480−10492

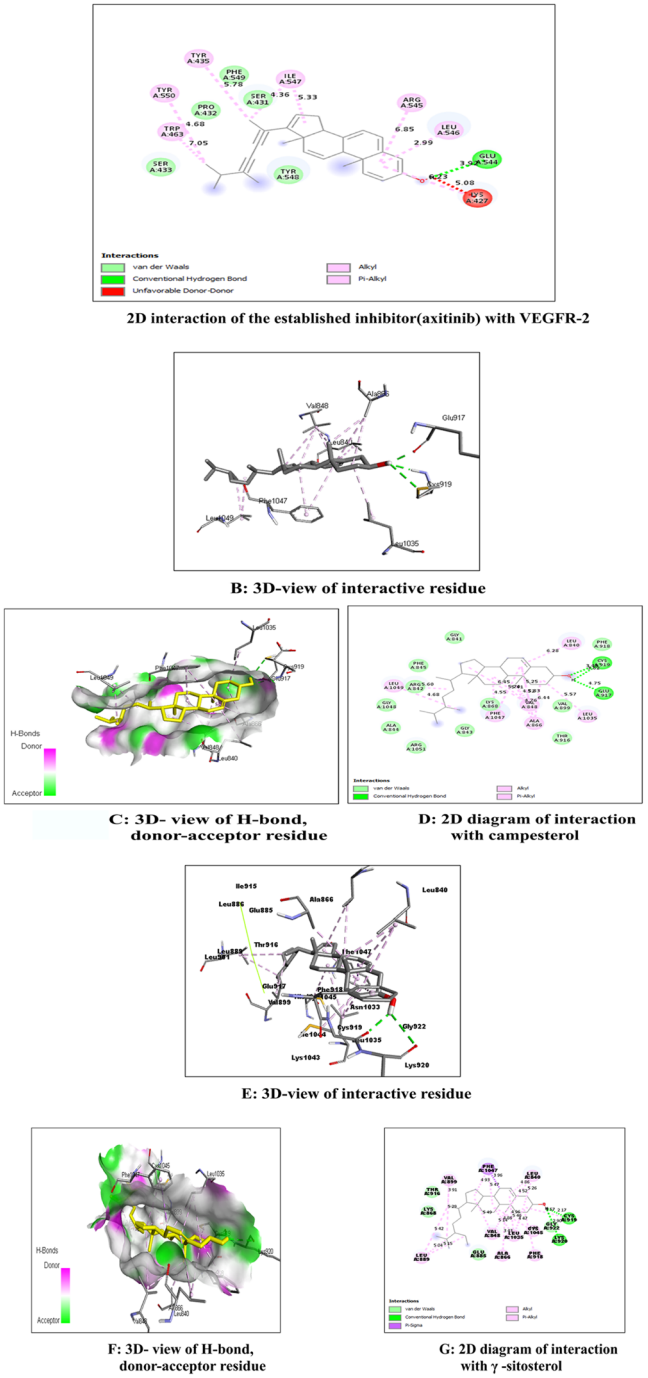

Figure 6. 3D and 2D interaction diagrams of the Campesterol and γ-sitosterol with their acceptor VEGFR2 (PDB: 3EWH).

VEGF receptors, VEGFR1, VEGFR2, and VEGFR3, exclusively.[65,66] Therefore, this drug served as the control for our bioinformatical docking studies. Molecular docking of campesterol and γ-sitosterol with all three VEGF receptors, VEGFR1, VEGFR2, and VEGFR3, indicates that these sterols may bind to the receptors at an affinity higher than that of axitinib. The binding energies of standard compound axitinib for VEGFR1, VEGFR2, and VEGFR3 were −9.50, −8.76, and −6.01 kcal/mol respectively. The binding energies of γ-sitosterol and campesterol for VEGFR-1 were −12.04 and −9.94 kcal/mol (Table 3) respectively, for VEGFR-2, −11.04 and −10.68 kcal/mol respectively (Table 4), and for VEGFR-3, −8.31 and −9.52 kcal/mol (Table 5) respectively, which indicates that the γ-sitosterol and campesterol have higher affinity toward VEGFR-1 (3HNG), VEGFR-2 (3EWH), and VEGFR-3 (4BSJ) than standard compound axitinib. This shows that γ-sitosterol and campesterol may block the ATP binding site and critical residue of VEGFR1 (Lys861 Glu878, Cys912, and Asp1040) (Figure 5) and VEGFR-2 (Lys868 Asp1046, Cys919, and Glu885) (Figure 6), thus enforcing their inhibitory effect.[38,39] It is possible that these substances effectively prevent angiogenesis by combining several methods, including the binding of VEGFR and the up-or-down-regulation of angiogenic proteins and genes. These naturally occurring substances could thus be potent angiogenesis inhibitors. For drug development, these sterols may serve as a lead compound to synthesize novel derivatives with improved binding properties to VEGF receptors. It was found that campesterol and γ-sitosterol obeyed Lipinski's rule of five (Table 6).[67,68] ADMET analysis was undertaken to understand better the bioactive compounds' pharmacokinetic properties (Table 7). Solubility, expressed as LogS, is an important property of drug-like compounds. The solubility of major bioactive compounds (−6.9 and −7.5) indicates their insoluble nature.[69] All compounds demonstrated positive results with regard to human intestine absorption (HIA). The blood-brain barrier (BBB) and colorectal cancer (Caco-2) have been investigated to determine membrane permeability.[70] All compounds have positive BBB and Caco-2 values, indicating that they can pass across the barriers. The compounds tested were found to be noninhibitors of Renal Organic Cation Transporter (ROCT) and substrates and inhibitors of P-glycoprotein, indicating drug distribution.[69] Because of its significance in Phase-I drug metabolism, cyto-chrome P450 (CYP450) is regarded as the main parameter used for examining ADME of pharmaceuticals.[71] According to the table, all compounds are neither substrates nor CYP450 inhibitors. The compounds were not associated with any toxicity issues, including hepatotoxicity or mutagenicity. All compounds tested negative for Salmonella/microsome mutagenicity assay (AMES), indicating that they were harmless (Figure 7). The results of the LD_{50} values and other toxicity hazards are presented in Table 7.

CONCLUSIONS

In vivo CAM experiment revealed that the ethyl acetate extract of parotoid gland secretion from the Indian common toad has significant antiangiogenic properties. This antiangiogenic action might be attributed by the presence of high amounts of sterol components. This discovery revealed a potential foundation for the use of an ethyl acetate extract of parotoid gland secretion to

Table 6. Drug-likeliness Properties of Major Sterols from Ethyl Acetate Extract of Parotoid Gland Secretion of Indian Common Toad

bioactive compounds	molecular weight	cLogP	cLogS	H acceptors	H donors	polar surface area	rotatable bonds
γ-sitosterol	414.72	5.07	−6.71	1	1	20.23	6
campesterol	400.68	4.92	−7.54	1	1	20.23	5

https://doi.org/10.1021/acsomega.4c10809
ACS Omega 2025, 10, 10480−10492

Table 7. Predicted ADMET Characteristics of the Main Sterols from Ethyl Acetate Extracts of the Parotoid Gland Secretion of the Indian Common Toad through SwissADME and pkCSM

compounds name	absorption		distribution			metabolism		excretion	toxicity		
bioactive compounds	Caco2 permeability (log Papp in 10^{-6} cm/s)	HIA (%)	VDss (log L/kg)	fraction unbound	BBB permeability (log BB)	CNS permeability (log PS)	CYP1A2 inhibitor	CYP3A4 substrate	total clearance (log mL/min/kg)	renal OCT2 substrate	hepatotoxicity	mutagenic	Oral rat acute toxicity (LD50) (mol/kg)
campesterol	1.223	95	0.43	0	0.77	−1.76	no	no	0.57	no	no	no	2.08
γ-sitosterol	1.201	94	0.19	0	0.78	−1.7	no	no	0.63	no	no	no	2.552

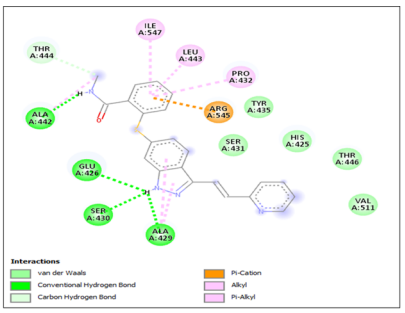

A: 2D interaction of the established inhibitor(axitinib) with VEGFR-3

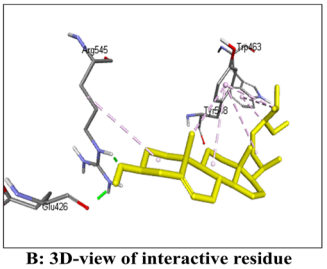

B: 3D-view of interactive residue γ-sitosterol with VEGFR-3

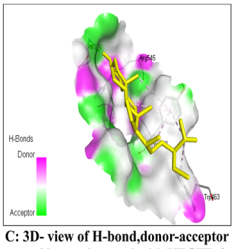

C: 3D- view of H-bond,donor-acceptor residue γ -sitosterol with VEGFR-3

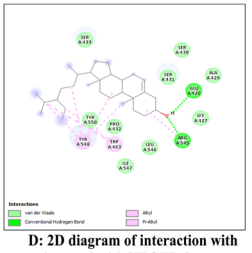

D: 2D diagram of interaction with γ -sitosterol with VEGFR-3

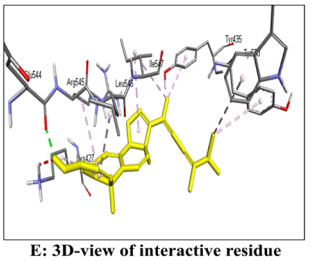

E: 3D-view of interactive residue campesterol with VEGFR-3

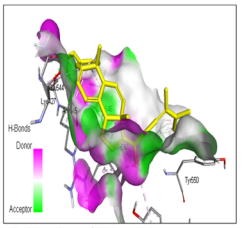

F: 3D- view of H-bond,donor-acceptor residue campesterol with VEGFR-3

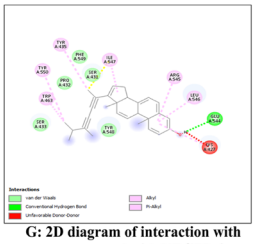

G: 2D diagram of interaction with campesterol with VEGFR-3

Figure 7. 3D and two-dimensional (2D) interaction diagrams of the campesterol and γ-sitosterol with their acceptor VEGFR3 (PDB-4BSJ).

prevent angiogenesis and a better treatment protocol for cancer. The findings might shed light on the pharmacological basis for the sterol-rich extract's traditional usage in effective cancer prevention.

Thus, the present study aims to evaluate the antiangiogenic activity of sterols derived from the parotoid secretions (PGS) by both the *in vivo and in silico* model of Indian common toad from the Indian subcontinent. In future, detail evaluation of all of the

https://doi.org/10.1021/acsomega.4c10809
ACS Omega 2025, 10, 10480−10492

different group of components present in parotoid gland secretions of *D. melanostictus*, in different model organism, help us to understand the details chemogenic and therapeutic role.

■ ASSOCIATED CONTENT

Supporting Information

The Supporting Information is available free of charge at https://pubs.acs.org/doi/10.1021/acsomega.4c10809.

Chorio-allantoic membrane assay, gas chromatography and mass spectrometry, half maximal effective concentration, vascular endothelial growth factor receptor, Ehrlich ascites carcinoma, etc (PDF)

3D and 2D interaction diagrams of the Campesterol and γ-sitosterol with their acceptor VEGFR1 (PDB 3HNG) (Figure S1); 3D and 2D interaction diagrams of the Campesterol and γ-sitosterol with their acceptor VEGFR2 (PDB 3EWH) (Figure S2); 3D and 2D interaction diagrams of the Campesterol and γ-sitosterol with their acceptor VEGFR3 (PDB 4BSJ) (Figure S3) (PDF)

Toad capture and sample collection (Figure S4) (PDF)

■ AUTHOR INFORMATION

Corresponding Authors

Sandhya Maji − *Research Scholar, Genetics and Molecular Biology Research Unit, Department of Zoology, Vidyasagar University, Paschim Medinipur, West Bengal 721102, India;* orcid.org/0009-0006-9444-9782; Phone: +918972022288; Email: sandhyamaji26@gmail.com

Jayanta Kumar Kundu − *Professor, Genetics and Molecular Biology Research Unit, Department of Zoology, Vidyasagar University, Paschim Medinipur, West Bengal 721102, India;* Phone: +919433126272; Email: jayantak62@gmail.com

Authors

Susanta Sadhukhan − *State Aided College Teacher-1, Bijoy Krishna Girl's College, Howrah, West Bengal 711101, India; Department of Zoology, University of Calcutta, Kolkata, West Bengal 700073, India*

Arup Kumar Pattanayak − *Molecular Biologist, Department of Microbiology, NRS Medical College, Kolkata, West Bengal 700014, India; Department of Zoology, University of Calcutta, Kolkata, West Bengal 700073, India;* orcid.org/0000-0001-8096-3023

Complete contact information is available at: https://pubs.acs.org/10.1021/acsomega.4c10809

Notes

The authors declare no competing financial interest.

■ ACKNOWLEDGMENTS

We would like to acknowledge University Grant Commission (UGC), Government of India for support.

■ REFERENCES

(1) Weidner, N.; Semple, J. P.; Welch, W. R.; Folkman, J. Tumor angiogenesis and metastasis-correlation in invasive breast carcinoma. *N. Engl. J. Med.* **1991**, *324* (1), 1−8.

(2) Cao, Y. Tumor angiogenesis and molecular targets for therapy. *Front. Biosci.* **2009**, 3962−3973.

(3) Carmeliet, P.; Jain, R. K. Molecular mechanisms and clinical applications of angiogenesis. *Nature* **2011**, *473* (7347), 298−307.

(4) Folkman, J.; Merler, E.; Abernathy, C.; Williams, G. Isolation of a Tumor Factor Responsible for Angiogenesis. *J. Exp. Med.* **1971**, *133*, 275−288.

(5) Newman, D. J.; Cragg, G. M. Natural products as sources of new drugs over the nearly four decades from 01/1981 to 09/2019. *J. Nat. Prod.* **2020**, *83* (3), 770−803.

(6) Yadav, L.; Puri, N.; Rastogi, V.; Satpute, P.; Sharma, V. Tumour angiogenesis and angiogenic inhibitors: a review. *J. Clin. Diagn. Res.* **2015**, *9* (6), No. XE01.

(7) Giri, B.; Gomes, A.; Debnath, A.; Saha, A.; Biswas, A. K.; Dasgupta, S. C.; Gomes, A. Antiproliferative, cytotoxic and apoptogenic activity of Indian toad (*B. melanostictus*, Schneider) skin extract on U937 and K562 cells. *Toxicon* **2006**, *48* (4), 388−400. Sep 15

(8) Frost, D. R. *Amphibian Species of the World: An Online Reference*, version 6.0; America n Museum of Natural History: New York, 2024.

(9) Alves, R. R. N.; Vieira, W. L.; Santana, G. G.; Vieira, K. S.; Montenegro, P. F. Herpetofauna Used in Traditional Folk Medicine: Conservation Implications. In *Animals in Traditional Folk Medicine: Implications for Conservation*; Springer, 2013; pp 109−133.

(10) Zhang, P.; Cui, Z.; Liu, Y.; Wang, D.; Liu, N.; Yoshikawa, M. Quality evaluation of traditional Chinese drug toad venom from different origins through a simultaneous determination of bufogenins and indole alkaloids by HPLC. *Chem. Pharm. Bull.* **2005**, *53* (12), 1582−1586.

(11) Zhang, Y.; Qiu, Y. K.; Chen, J. Y.; Bo, K. N.; Jiang, Y. T.; Pei, Y. H. Chemical constituents from the skin of *Bufobufogargarizans* Cantor. *J. Shenyang Pharm. Univ.* **2007**, *8*, 484−487.

(12) Zhao, H.; Wu, X.; Wang, H.; Gao, B.; Yang, J.; Si, N.; Bian, B. Determination of eight bufadienolides in the skin of *Bufobufogargarizans* Cantor and *B. melanostictus* Schneider using HPLC coupled with triple quadrupole mass spectrometry. *J. Liq. Chromatogr. Relat. Technol.* **2014**, *37* (8), 1163−1175.

(13) Zhao, H. Y.; Wu, F. K.; Qiu, Y. K.; Wu, Z.; Jiang, Y. T.; Chen, J. Y. Studies on cytotoxic constituents from the skin of the toad *Bufobufogargarizans*. *J. Asian Nat. Prod. Res.* **2010**, *12* (9), 793−800.

(14) Verpoorte, R.; Svendsen, A. B. Chemical constituents of Vietnamese toad venom collected from *Bufomelanostictus* Schneider: Part I. The sterols. *J. Ethnopharmacol.* **1979**, *1* (2), 197−202.

(15) Wang, Y. M.; Li, Z. Y.; Wang, J. J.; Wu, X. Y.; Gao, H. M.; Wang, Z. M. Bufadienolides and polyhydroxy cholestane derivatives from *Bufobufogargarizans*. *J. Asian Nat. Prod. Res.* **2015**, *17* (4), 364−376.

(16) Shimada, K.; Ohishi, K.; Nambara, T. Isolation and characterization of new bufotoxins from the skin of *B. melanostictus* Schneider. *Chem. Pharm. Bull.* **1984**, *32* (11), 4396−4401.

(17) Shimada, K.; Ro, J. S.; Kanno, C.; Nambara, T. Occurrence of bufogenin conjugates in the skin of Korean toad. *Chem. Pharm. Bull.* **1987**, *35* (12), 4996−4999.

(18) Shimada, K.; Ro, J.; Ohishi, K.; Nambara, T. Isolation and characterization of cinobufagin 3-glutaroyl-L-arginine ester from *Bufobufogargarizans* Cantor. *Chem. Pharm. Bull.* **1985**, *33* (7), 2767−2771.

(19) Shimada, K.; Sato, Y.; Fujii, Y.; Nambara, T. Occurrence of bufalitoxin, cinobufotoxin and their homologs in Japanese toad. *Chem. Pharm. Bull.* **1976**, *24* (5), 1118−1120.

(20) Li, H. Y.; Zhang, L. Z.; Wang, S. H.; Deng, Y.; Jin, X. Q. Two new bufotoxins from the skin of *Bufobufogargarizans*. *Chin. Chem. Lett.* **2013**, *24* (8), 731−733.

(21) Li, X.; Guo, Z.; Wang, C.; Shen, A.; Liu, Y.; Zhang, X.; Zhao, W.; Liang, X. Purification of bufadienolides from the skin of *Bufobufogargarizans* Cantor with positively charged C18 column. *J. Pharm. Biomed. Anal.* **2014**, *92*, 105−113.

(22) Liu, C.; Cao, W.; Chen, Y.; Qu, D.; Zhou, J. Comparison of toad skins *Bufobufogargarizans* Cantor from different regions for their active constituents content and cytotoxic activity on lung carcinoma cell lines. *Pharmacogn. Mag.* **2014**, *10* (39), 207.

(23) Liu, J.; Zhang, D.; Li, Y.; Chen, W.; Ruan, Z.; Deng, L.; Wang, L.; Tian, H.; Yiu, A.; Fan, C.; Luo, H.; et al. Discovery of bufadienolides as a novel class of ClC-3 chloride channel activators with antitumor activities. *J. Med. Chem.* **2013**, *56* (14), 5734−5743.

(24) Liu, Y.; Feng, J.; Xiao, Y.; Guo, Z.; Zhang, J.; Xue, X.; Ding, J.; Zhang, X.; Liang, X. Purification of active bufadienolides from toad skin by preparative reversed-phase liquid chromatography coupled with hydrophilic interaction chromatography. *J. Sep. Sci.* **2010**, *33* (10), 1487−1494.
(25) Liu, Y.; Xiao, Y.; Xue, X.; Zhang, X.; Liang, X. Systematic screening and characterization of novel bufadienolides from toad skin using ultra-performance liquid chromatography/electrospray ionization quadrupole time-of-flight mass spectrometry. *Rapid Commun. Mass Spectrom.* **2010**, *24* (5), 667−678.
(26) Perera Córdova, W. H.; Leitão, S. G.; Cunha-Filho, G.; Bosch, R. A.; Alonso, I. P.; Pereda-Miranda, R.; Gervou, R.; Touza, N. A.; Quintas, L. E.; Noël, F. Bufadienolides from parotoid gland secretions of Cuban toad *Peltophrynefustiger* (Bufonidae): inhibition of human kidney Na+/K+-ATPase activity. *Toxicon* **2016**, *110*, 27−34.
(27) Das, M.; Dasgupta, S. C.; Gomes, A. Immunomodulatory and antineoplastic activity of common Indian toad (*Bufo melanostictus*, Schneider) skin extract. *Indian J. Pharmacol.* **1998**, *30* (5), 311−317.
(28) Gomes, A.; Giri, B.; Alam, A.; Mukherjee, S.; Bhattacharjee, P.; Gomes, A. Anticancer activity of a low immunogenic protein toxin (BMP1) from Indian toad (*Bufo melanostictus*, Schneider) skin extract. *Toxicon* **2011**, *58* (1), 85−92.
(29) Bhattacharjee, P.; Giri, B.; Gomes, A. Apoptogenic activity and toxicity studies of a cytotoxic protein (BMP1) from the aqueous extract of common Indian toad (*Bufo melanostictus* Schneider) skin. *Toxicon* **2011**, *57* (2), 225−236.
(30) Peifer, C.; Dannhardt, G. A novel quantitative chick embryo assay as an angiogenesis model using digital image analysis. *Anticancer Res.* **2004**, *24* (3), 1545−1552.
(31) Ribatti, D. Chicken Chorioallantoic Membrane Angiogenesis Model. In *Cardiovascular Development: Methods and Protocols*; Springer, 2012; Vol. *843*, pp 47−57.
(32) Avram, Ş.; Cimpean, A. M.; Raica, M. Behavior of the P1. HTR mastocytoma cell line implanted in the chorioallantoic membrane of chick embryos. *Braz. J. Med. Biol. Res.* **2013**, *46* (1), 52−57.
(33) Morris, G. M.; Huey, R.; Lindstrom, W.; Sanner, M. F.; Belew, R. K.; Goodsell, D. S.; Olson, A. J. AutoDock4 and AutoDockTools4: Automated docking with selective receptor flexibility. *J. Comput. Chem.* **2009**, *30* (16), 2785−2791.
(34) Tresaugues, L.; Roos, A.; Arrowsmith, C.; Berglund, H.; Bountra, C.; Collins, R.; Edwards, A. M.; Flodin, S.; Flores, A.; Graslund, S.; Hammarstrom, M. Crystal structure of VEGFR1 in complex with N-(4-Chlorophenyl)-2-((pyridin-4-ylmethyl)amino)benzamide *RCSB PDB* 2013.
(35) Cee, V. J.; Cheng, A. C.; Romero, K.; Bellon, S.; Mohr, C.; Whittington, D. A.; Bak, A.; Bready, J.; Caenepeel, S.; Coxon, A.; Deak, H. L.; et al. Pyridyl-pyrimidine benzimidazole derivatives as potent, selective, and orally bioavailable inhibitors of Tie-2 kinase. *Bioorg. Med. Chem. Lett.* **2009**, *19* (2), 424−427.
(36) Leppänen, V.-M.; Tvorogov, D.; Kisko, K.; Prota, A. E.; Jeltsch, M.; Anisimov, A.; Markovic-Mueller, S.; Stuttfeld, E.; Goldie, K. N.; Ballmer-Hofer, K.; Alitalo, K. Structural and mechanistic insights into VEGF receptor 3 ligand binding and activation. *Proc. Natl. Acad. Sci. U.S.A.* **2013**, *110* (32), 12960−12965.
(37) O'Boyle, N. M.; Banck, M.; James, C. A.; Morley, C.; Vandermeersch, T.; Hutchison, G. R. Open Babel: An open chemical toolbox. *J. Cheminf.* **2011**, *3*, 1−4.
(38) Morris, G. M.; Goodsell, D. S.; Halliday, R. S.; Huey, R.; Hart, W. E.; Belew, R. K.; Olson, A. J. Automated docking using a Lamarckian genetic algorithm and an empirical binding free energy function. *J. Comput. Chem.* **1998**, *19* (14), 1639−1662.
(39) Pettersen, E. F.; Goddard, T. D.; Huang, C. C.; Couch, G. S.; Greenblatt, D. M.; Meng, E. C.; Ferrin, T. E. UCSF Chimera—a visualization system for exploratory research and analysis. *J. Comput. Chem.* **2004**, *25* (13), 1605−1612.
(40) Daina, A.; Michielin, O.; Zoete, V. SwissADME: a free web tool to evaluate pharmacokinetics, drug-likeness and medicinal chemistry friendliness of small molecules. *Sci. Rep.* **2017**, *7* (1), No. 42717.
(41) Pires, D. E. V.; Blundell, T. L.; Ascher, D. B. pkCSM: predicting small-molecule pharmacokinetic and toxicity properties using graph-based signatures. *J. Med. Chem.* **2015**, *58* (9), 4066−4072.
(42) Cheng, F.; Yu, Y.; Zhou, Y.; Shen, Z.; Xiao, W.; Liu, G.; Li, W.; Lee, P.; Tang, Y. Insights into the molecular basis of cytochrome P450 inhibitory promiscuity of compounds. *J. Chem. Inf. Model.* **2011**, *51* (10), 2482−2495.
(43) Zhang, Y.; Chen, Y.; Zhang, D.; Wang, L.; Lu, T.; Jiao, Y. Discovery of novel potent VEGFR-2 inhibitors exerting significant antiproliferative activity against cancer cell lines. *J. Med. Chem.* **2018**, *61* (1), 140−157.
(44) Asthana, S.; Agarwal, T.; Singothu, S.; Samal, A.; Banerjee, I.; Pal, K.; Pramanik, K.; Ray, S. S. Molecular docking and interactions of *puerariatuberosa* with vascular endothelial growth factor receptors. *Indian J. Pharm. Sci.* **2015**, *77* (4), 439.
(45) Gao, H.; Zehl, M.; Leitner, A.; Wu, X.; Wang, Z.; Kopp, B. Comparison of toad venoms from different Bufo species by HPLC and LC-DAD-MS/MS. *J. Ethnopharmacol.* **2010**, *131* (2), 368−376.
(46) Yoshii, M.; Une, M.; Kihira, K.; Kuramoto, T.; Akizawa, T.; Yoshioka, M.; Butler, Jr V. P.; Hoshita, T. Bile salts of the toad, Bufo marinus: characterization of a new unsaturated higher bile acid, 3 alpha, 7 alpha, 12 alpha, 26-tetrahydroxy-5 beta-cholest-23-en-27-oic acid. *J. Lipid Res.* **1994**, *35* (9), 1646−1651.
(47) Une, M.; Kuramoto, T.; Hoshita, T. The minor bile acids of the toad, *Bufo vulgaris* formosus. *J. Lipid Res.* **1983**, *24* (11), 1468−1474.
(48) Hüttel, R.; Behringer, H. The occurrence of plant sterols in toads. *Z. Physiol. Chem.* **1937**, *245*, 175.
(49) Beadle, G. W.; Brauns, F. E.; Deulofeu, V.; Doudoroff, M.; Fox, D. L.; Geiger, E.; Haagen-Smith, A. J.; Hassid, W. Z.; Hilditch, T. P.; Karrer, P.; Pacsu, E. The chemistry of the constituents of toad venoms. *Fortschr. Chem. organisch. Naturstoffe* **1948**, 241−266.
(50) Meyer, K.; Linde, H. Collection of toad venoms and chemistry of the toad venom steroids. *Venomous Anim. Their Venoms* **1971**, 521−556.
(51) Rees, R.; Schindler, O.; Deulofeu, V.; Reichstein, T. Die Bufogenine des Paratoidensekretes von Bufoarenarum HENSEL. ÜberKrötengifte, 20. Mitteilung. *Helv. Chim. Acta* **1959**, *42* (7), 2400−2418.
(52) Rajani Mathur, R. M.; Gupta, S. K.; Neeta Singh, N. S.; Sandeep Mathur, S. M.; Vinod Kochupillai, V. K.; ThirumurthyVelpandian, T. V. Evaluation of the effect of Withaniasomnifera root extracts on cell cycle and angiogenesis. *J. Ethnopharmacol.* **2006**, *105*, 336−341.
(53) Sundarraj, S.; Thangam, R.; Sreevani, V.; Kaveri, K.; Gunasekaran, P.; Achiraman, S.; Kannan, S. γ-Sitosterol from Acacia nilotica L. induces G2/M cell cycle arrest and apoptosis through c-Myc suppression in MCF-7 and A549 cells. *J. Ethnopharmacol.* **2012**, *141* (3), 803−809.
(54) Marinangeli, C. P.; Varady, K. A.; Jones, P. J. Plant sterols combined with exercise for the treatment of hypercholesterolemia: an overview of independent and synergistic mechanisms of action. *J. Nutr. Biochem.* **2006**, *17* (4), 217−224.
(55) Endrini, S.; Rahmat, A.; Ismail, P.; Taufiq-Yap, Y. H. Cytotoxic effect of γ-sitosterol from Kejibeling (*Strobilanthescrispus*) and its mechanism of action towards c-myc gene expression and apoptotic pathway. *Med. J. Indonesia* **2015**, *23* (4), 203−208.
(56) Woyengo, T. A.; Ramprasath, V. R.; Jones, P. J. Anticancer effects of phytosterols. *Eur. J. Clin. Nutr.* **2009**, *63* (7), 813−820.
(57) Bradford, P. G.; Awad, A. B. Phytosterols as anticancer compounds. *Mol. Nutr. Food Res.* **2007**, *51* (2), 161−170.
(58) Andrade, J. C.; Braga, M. F.; Guedes, G. M.; Tintino, S. R.; Freitas, M. A.; Quintans, L. J.; Menezes, I. R.; Coutinho, H. D. Cholecalciferol, ergosterol, and cholesterol enhance the antibiotic activity of drugs. *Int. J. Vitam. Nutr. Res.* **2018**, *39*, 244−250.
(59) Dinku, W.; Choi, S. U.; Lee, S.-H.; Jung, Y.-S.; No, Z. S.; Dekebo, A. Antiproliferative Effect of Sterols from Resin of Commiphorahabessinica. *J. Pharm. Nutr. Sci.* **2019**, *9* (2), 71−80.
(60) Seo, E. J.; Kuete, V.; Kadioglu, O.; Krusche, B.; Schröder, S.; Greten, H. J.; Arend, J.; Lee, I. S.; Efferth, T. Antiangiogenic activity and pharmacogenomics of medicinal plants from traditional Korean

https://doi.org/10.1021/acsomega.4c10809
ACS Omega 2025, 10, 10480−10492

medicine. *Evidence-Based Complementary Altern. Med.* **2013**, *2013* (1), No. 131306.
(61) Nayarisseri, A.; Abdalla, M.; Joshi, I.; Yadav, M.; Bhrdwaj, A.; Chopra, I.; Khan, A.; Saxena, A.; Sharma, K.; Panicker, A.; Panwar, U.; et al. Potential inhibitors of VEGFR1, VEGFR2, and VEGFR3 developed through Deep Learning for the treatment of Cervical Cancer. *Sci. Rep.* **2024**, *14* (1), No. 13251.
(62) Neufeld, G.; Cohen, T.; Gengrinovitch, S.; Poltorak, Z. Vascular endothelial growth factor (VEGF) and its receptors. *FASEB J.* **1999**, *13* (1), 9−22.
(63) Roskoski, R., Jr VEGF receptor protein−tyrosine kinases: structure and regulation. *Biochem. Biophys. Res. Commun.* **2008**, *375* (3), 287−291.
(64) Ji, L.; Wu, M.; Li, Z. Rutacecarpine inhibits angiogenesis by targeting the VEGFR2 and VEGFR2-mediated Akt/mTOR/p70s6k signalling pathway. *Molecules* **2018**, *23* (8), 2047.
(65) Choueiri, T. K. Axitinib is a novel anti-angiogenic drug with promising activity in various solid tumors. *Curr. Opin. Invest. Drugs* **2008**, *9* (6), 658−671.
(66) Kelly, R. J.; Rixe, O. Axitinib—a selective inhibitor of the vascular endothelial growth factor (VEGF) receptor. *Target. Oncol.* **2009**, *4*, 297−305.
(67) Lipinski, C. A. Lead-and drug-like compounds: the rule-of-fiverevolution. *Drug Discovery Today Technol.* **2004**, *1* (4), 337−341.
(68) Lipinski, C. A. Rule of five in 2015 and beyond target and ligandstructural limitations, ligand chemistry structure and drug discoveryproject decisions. *Adv. Drug Delivery Rev.* **2016**, *101*, 34−41.
(69) Joshi, T.; Joshi, T.; Sharma, P.; Pundir, H.; Chandra, S. In silico identification of natural fungicide from Melia azedarach against isocitrate lyase of *Fusarium graminearum*. *J. Biomol. Struct. Dyn.* **2021**, *39* (13), 4816−4834.
(70) Niveshika; Singh, S.; Verma, E.; Mishra, A. K. In silico molecular docking analysis of cancer biomarkers with GC/MS identified compounds of Scytonema sp. *Netw. Model. Anal. Health Inform. Bioinform.* **2020**, *9*, 1−4.
(71) Paramashivam, S. K.; Elayaperumal, K.; bhagavan Natarajan, B.; deviRamamoorthy, M.; Balasubramanian, S.; Dhiraviam, K. N. In silico pharmacokinetic and molecular docking studies of small molecules derived from Indigoferaaspalathoides Vahl targeting receptor tyrosine kinases. *Bioinformation* **2015**, *11* (2), 73.
(72) Abeywardhana, S.; Premathilaka, M.; Bandaranayake, U.; Perera, D.; Peiris, L. D. In silico study of SARS-CoV-2 spike protein RBD and human ACE-2 affinity dynamics across variants and Omicron subvariants. *J. Med. Virol.* **2023**, *95* (1), No. e28406.

https://doi.org/10.1021/acsomega.4c10809
ACS Omega 2025, 10, 10480−10492